ACS OMEGA

http://pubs.acs.org/journal/acsodf

Article

Assessment of Eggshell Membrane as a New Type of Proton-Conductive Membrane in Fuel Cells

Naoki Tanifuji,* Takeshi Shimizu,* Hirofumi Yoshikawa, Miki Tanaka, Kosuke Nishio, Kentaro Ida, Akihiro Shimizu, and Yukio Hasebe

Cite This: *ACS Omega* 2022, 7, 12637−12642

Read Online

ACCESS | Metrics & More | Article Recommendations | Supporting Information

ABSTRACT: Polymer electrolyte membrane fuel cells have recently attracted considerable attention as sustainable and eco-friendly electricity generation devices from the viewpoint of carbon neutrality. This study focuses on new discoveries related to the application of eggshell membranes to polymer electrolytes in the development of cheaper, more eco-friendly fuel cells. We observed the electricity generation of the fuel cells using an eggshell membrane as a proton-conductive material and a general carbonic acid aqueous solution. This new fuel cell will contribute to the continued improvement of available fuel cells at lower costs.

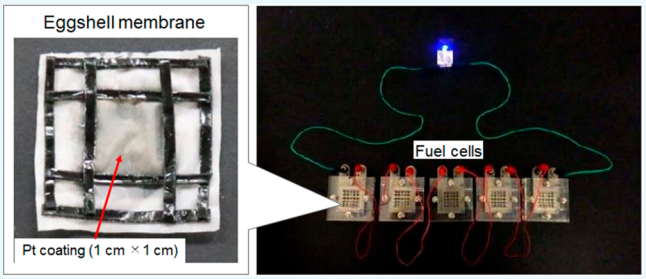

INTRODUCTION

Recently, renewable energy systems have been developed to reduce carbon dioxide emissions as part of a global effort to achieve carbon neutrality. Among these techniques, polymer electrolyte membrane fuel cell (PEFC) technologies, which generate electric energy via proton generation supported by a Pt catalyst on the cathode, proton conduction through the polymer membrane, and water generation by the combination of protons with oxygen on the anode,[1] have been most widely employed for energy loss reduction in both household[2] and automotive[3,4] applications. Conventional PEFCs contain Nafion, a perfluorosulfonic acid polymer membrane developed by DuPont, as proton-conductive membranes and exhibit a proton conductivity of 1×10^{-1} S cm^{-1}, even at 70−90 °C under hydrous conditions. However, new membranes substituted for Nafion require wider testing, because conventional PEFC with Nafion has low thermal stability (glass transition temperature of Nafion is approximately 100 °C) and requires soaking in strong acid. The polymer is also environmentally burdensome due to combustion.[5] Therefore, we explored a new candidate for PEFC membrane to meet above demands.

In this study, we employed a chicken eggshell membrane as the PEFC membrane. The eggshell membrane is nanoporous, is thinner than other avian membranes,[6−8] and is composed of insoluble protein fibers abundant in amines and amides,[9] offering proton conductivity without crossover of fuel. In addition, eggshell membranes have high thermal stability, CO_2 absorption,[10] and excellent eco-friendly recyclability for use in cosmetics, fertilizers, and food processing. Therefore, they show promise as PEFC membranes due to their cost-effectiveness and easy availability as organic support materials. This work reports the development of a fuel cell utilizing a carbonic acid aqueous solution as a new fuel supplement for electricity generation and describes the fabrication of a new solid electrolyte comprising an eggshell membrane, showing that the amount of generated electricity is sufficient for lighting up red and blue LEDs.

RESULTS AND DISCUSSION

First, thermogravimetric analysis was conducted to evaluate the thermal stability of the eggshell membrane. Figure 1 shows thermogravimetric (TG), differential thermal analysis (DTA), and derivative TG (DTG) curves of the eggshell membrane. The initial mass loss of approximately 10% observed in the TG curve was ascribed to moisture evaporation, and TG and DTG showed a constant mass area corresponding to the thermal stability region of the eggshell membrane protein (<250 °C). The DTA curve showed an endothermic peak at 340 °C, corresponding to eggshell membrane degradation, although no endothermic peak was derived from denaturation. Furthermore, differential scanning calorimetry (DSC, Figure S1) shows no peaks ascribed to glass transition between 30−230 °C. These results indicate that this membrane has novel thermal stability.[11]

Next, the structural stability of the eggshell membrane was investigated by using IR measurement. Figure S2 reveals a broad peak (amine, 3200−3500 cm^{-1}),[9] two distinct peaks

Received: November 26, 2021
Accepted: March 31, 2022
Published: April 11, 2022

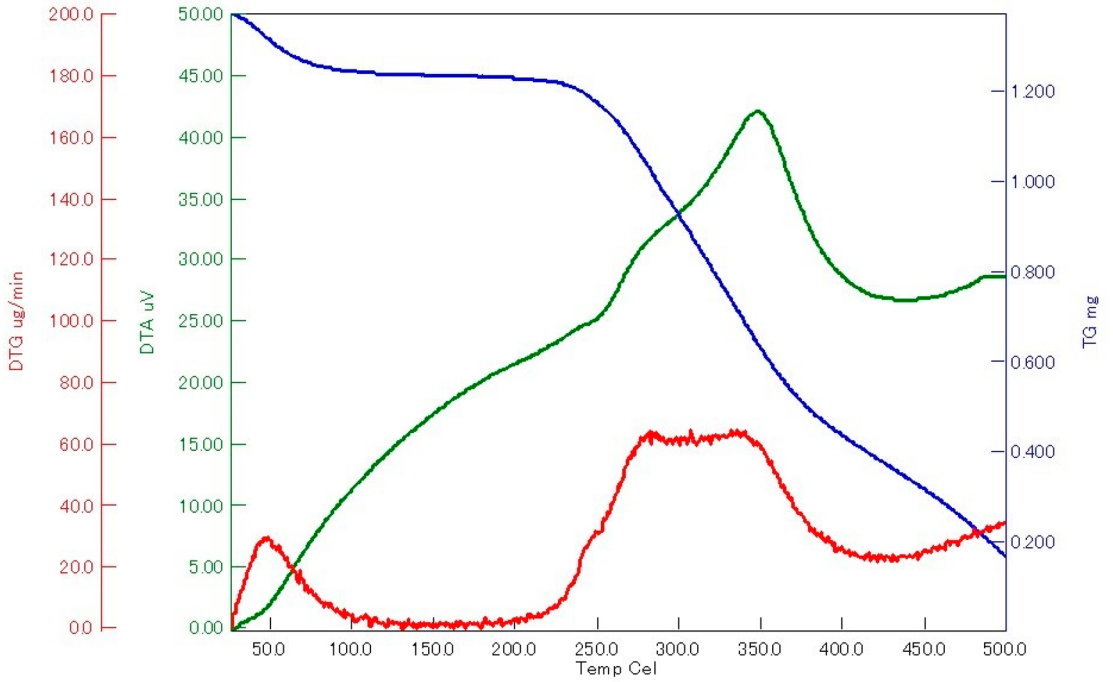

Figure 1. TG (blue), DTA (green), and DTG (red) curves of the eggshell membrane.

(amide, 1652 and 1385 cm^{-1}),[9] and another single peak (S−C in cystine, 661 cm^{-1}).[12] Signals were also observed at 4.824, 3.780, and 1.263 ppm in the ^{1}H MAS spectrum, indicating that hydrogen-bonding protons[13,14] in water were present in the eggshell membrane (Figure S3). In addition, peaks were attributed to cystine (37−43 ppm),[15] lipids (51.91 and 58.03 ppm),[16] and carbonyl groups of proteins (172.14 ppm)[16] in the ^{13}C CP MAS spectrum (Figure S4). Therefore, the structural order of the eggshell membrane was maintained by hydrogen bonding and cystine.[15] This means that the structural stability originating from the S−S bonds in the cystine and side chain hydrogen bonding greatly contributes to the secondary and tertiary structure of proteins.[15] These side chains, such as carboxylate groups of aspartic acid and glutamic acid,[17] are expected to function as proton migration sites.[18] Moreover, the diffusion reflectance spectrum (Figure S5) was similar to that previously reported.[19] These results mean that the membrane was obtained without damage or denaturation.

Finally, the morphologies of the eggshell membrane were observed by scanning electron microscopy (SEM). Figure S6a,b suggests that the eggshell membrane structure was maintained after Pt-coating, and the thickness of the membrane was ca. 40 μm (Figure S6c,d), which was smaller than that of the ostrich eggshell membrane (ca. 100 μm).[8] According to the energy dispersive X-ray (EDX, Figure S6e,f) spectrum, no calcium was observed on the eggshell membrane due to removal of $CaCO_3$ by acetic acid. However, Pt catalyst on the eggshell membrane could not be observed because of low loading (30 $\mu g\ cm^{-2}$). In addition, the nanosized pores were too small to observe,[20] indicating that the tiny pores could generate electricity stably because of prevention of crossover.

Performances of the Eggshell Membrane for Electric Power Generation. Figure 2a shows a Pt-coated eggshell membrane, in which the center (1 cm × 1 cm) can generate electricity by supporting the Pt coating on the membrane. As shown in Figure 2b, electricity was generated in the Pt-coated

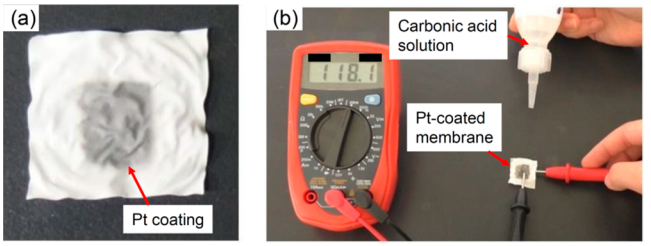

Figure 2. Pt-coated membrane (a) and preliminary testing for electricity generation (b).

membrane, absorbing a few drops of aqueous carbonic acid solution without dissolution. Moreover, the eggshell membranes immersed in pure water showed a proton conductivity σ of 1.4 × 10^{-4} S cm^{-1}, although the conductivity of the dry eggshell membrane was 7.3 × 10^{-5} S cm^{-1} (Figure 3). These conductivities were lower than those of the hydrophilic proton conductive materials (sulfonated ostrich eggshell membrane, 4.8 × 10^{-2} S cm^{-1};[21] cellulose nanofiber membrane, 8 × 10^{-4} S cm^{-1};[22] and Nafion membrane, 7.8 × 10^{-2} S cm^{-1} at RH 80%, ∼10^{-3} S cm^{-1} at RH 20%[23,24]) because of the hydrophobicity of the eggshell membrane.[25] However, the conductivities of eggshell membranes were higher than that of a cellulose nanocrystal membrane (5 × 10^{-5} S cm^{-1}).[22]

Power Generation Performance of the Fuel Cells Using the Eggshell Membrane. Figure 4a,b shows the $I-V$ curves and the power generation performance of the fuel cells using the eggshell membrane under the effects of the operating temperature (5−35 °C). This demonstrates that the rate of the electricity-generation-responsible reaction, and hence the efficiency of electricity generation, increased with increasing temperature. In addition, the power of the cell gradually decreased from the initial level of 20 $\mu W/cm^2$ to 5 $\mu W/cm^2$ after 30 days, indicating that the durability was sufficient for fuel cells.

https://doi.org/10.1021/acsomega.1c06687
ACS Omega 2022, 7, 12637−12642

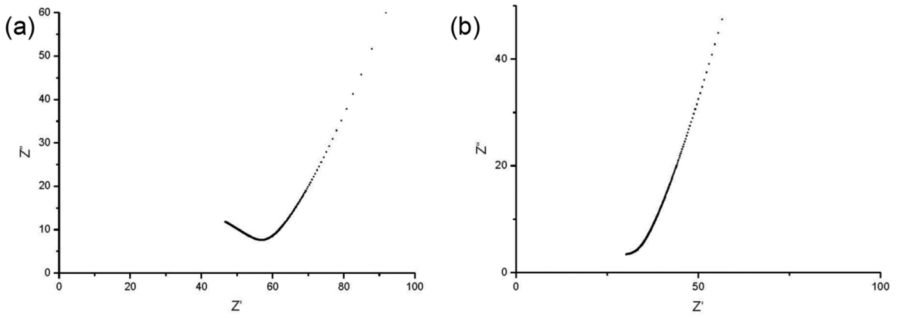

Figure 3. Proton conductivity measurement of eggshell membranes. Pt-coated eggshell membrane before (a) and after (b) soaking in pure water.

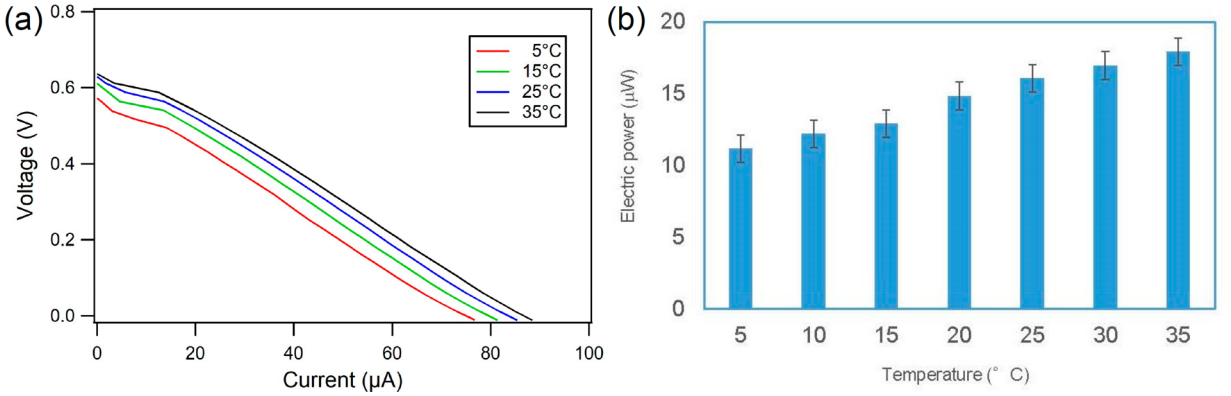

Figure 4. (a) *I*−*V* curves of the fuel cell using a Pt-coated eggshell membrane as an electrolyte membrane at four operating temperatures (5, 15, 25, and 35 °C). (b) The effect of operation temperatures (5, 10, 15, 20, 25, 30, and 35 °C) on electricity generation performance.

Next, the fuel cell using a carbonic acid aqueous solution showed the effect of Ar/air switching on electric power generation. As shown in Figure 5, the fuel cells exhibited

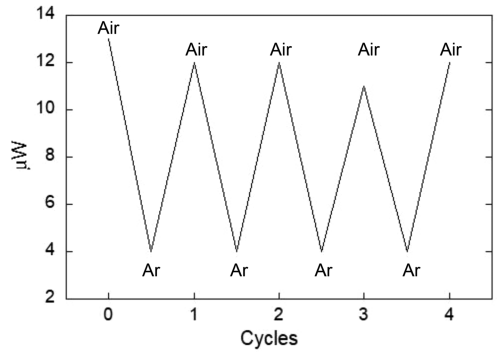

Figure 5. Effect of Ar/air switching on electric power generation.

powers of 11−13 μW in air. However, the power declined to 4 μW under the Ar flow. In this case, the power declined to 4 μW upon Ar introduction, likely because a small amount of oxygen generated at the anode passed through the membrane and reached the cathode. We explained a plausible mechanism based on these results (eqs 1−3):

$$\text{Anode: } H_2CO_3 \rightarrow 1/2O_2 + CO_2 + 2H^+ + 2e^- \quad (1)$$

$$\text{Cathode: } 2H^+ + 1/2O_2 + 2e^- \rightarrow H_2O \quad (2)$$

$$\text{Total: } H_2CO_3 \rightarrow CO_2 + H_2O \quad (3)$$

Proton, produced by the conversion of carbonic acid H_2CO_3 as fuel at the anode, was conducted through the eggshell membrane toward the cathode. At the cathode, proton and oxygen converted into H_2O in the presence of air flow. Although CO_2 was not directly involved in the chemical reaction and electricity generation, CO_2 dissolved in the aqueous solution increased its reactivity toward the catalyst, resulting in electricity generation. We suggest that the hydroxyl groups of carbonic acid coordinate to the metal catalyst, followed by proton detachment and electron migration.

The efficiency of electricity generation was not high because the Pt coverage area and loading were only 1 cm^2 and 30 μg, respectively.[26] However, three and five units in series could exhibit a voltage sufficient to light up red and blue LEDs for 30 days, respectively, based on the fact that a voltage of ∼0.8 V per unit could be achieved (Figure 6).

CONCLUSION

In conclusion, although the electricity generation of the eggshell membrane was lower than that of Nafion, our new fuel cells may contribute to the development of devices such as electric vehicles,[27] from the viewpoint of availability, low cost, and eco-friendliness. However, the PEFC with the eggshell membrane generated lower power density than PEFC with Nafion. This was caused by the small-sized cells and a small amount of Pt catalyst (30 μg cm^{-2}). In the case of Nafion, 1 g of Pt catalyst could be loaded on the membrane because of the plasticity of Nafion. We will fabricate a Pt-coated eggshell membrane/Nafion composite by hot-pressing Nafion with a high loading of Pt catalyst onto the eggshell membrane. Also, we will prove the detailed electricity generation mechanism of the fuel cells using carbonic acid by time-resolved Pt L_{III}-edge

https://doi.org/10.1021/acsomega.1c06687
ACS Omega 2022, 7, 12637−12642

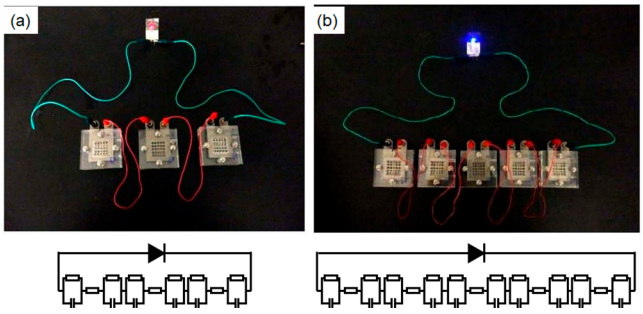

Figure 6. LED operation enabled by direct carbonic acid−mediated electricity generation. (a) A red LED (forward voltage V_F = 2.0 V, forward current I_F = 20 mA), and blue LED (V_F = 3.2 V, I_F = 20 mA) lit up by three and five cells in series, respectively. The equivalent circuits were assumed below (a) and (b), respectively.

X-ray absorption fine structure (XAFS) and *in situ* IR measurements as future work.[28] In the future, we intend to further improve the device structure to be suitable for quick electricity generation in emergencies from available carbonic acid aqueous solutions. Also, the cost to assemble a fuel cell using an eggshell membrane was just 0.2 cents per unit, and a larger eggshell membrane, such as ostrich eggs, can be used for upscaling purposes. We believe that these advantages will contribute to the development of fuel cells at lower costs.

EXPERIMENTAL METHODS

Materials. All materials were used without further purification. Acetic acid (99.7%) was purchased from Kishida Chemical Co. Ltd. Wilkinson Tansan and carbon dioxide were purchased from Asahi Soft Drinks Co., Ltd. and were used as carbonic acid solution.

Preparation of the Eggshell Membrane. The liquid content was first removed through a hole in the tip of a chicken egg, and the empty eggshell with the membrane was immersed in 30 wt % acetic acid aqueous solution for 1 day to dissolve only the calcium carbonate shell (Figure S7a). Next, the top and bottom of the membrane were cut off to leave a flat rectangular area in the equatorial plane of the egg (Figure S7b), while four square and flat membranes (3 cm × 3 cm) were obtained using an acrylic resin template (Figure S7c). Finally, the membranes were dried at room temperature (Figure S7d). To characterize the membrane, we conducted TGA, infrared, and diffuse-reflectance ultraviolet (UV) spectroscopy using a dry eggshell membrane. TGA was carried out with TG/DTA7300 (HITACHI) from 30 to 500 °C at a heating rate of 5 °C min^{-1} under N_2. DSC was conducted on DSC7020 (HITACHI) from 30 to 300 °C at a heating rate of 5 °C min^{-1} under N_2. Infrared (IR) measurements were carried out using an FT/IR-4100 instrument (Jasco). The IR light irradiated on the membrane was measured in the wavenumber region of 4000−500 cm^{-1} in air. Diffuse reflectance UV spectroscopy was performed using a UV-3600 UV−vis−NIR spectrophotometer (Shimadzu) in air.

A Pt sputter coating was applied to both sides of the eggshell membrane using magnetron sputtering equipment and a Pt target. For coating, Pt (30 $\mu g/cm^2$) was applied to both sides of the membrane using an acrylic template with a 1 cm × 1 cm square hole for 1 min. The voltage across the Pt-coated membrane was confirmed with a multimeter when several drops of carbonic acid aqueous solution were added to one side of the membrane.

Scanning Electron Microscopy (SEM) Equipped with Energy Dispersive X-ray Spectroscopy (EDX) Characterization. SEM was performed on JCM-6610 (JEOL), where the voltage was set to 15 kV. The samples on carbon tapes were sputtered with gold in vacuo for 2 min and three times, and then SEM images of samples were taken under high vacuum. EDX was performed with a silicon drift detector (JED-2300, JEOL) energy dispersive spectrometer equipped with SEM.

Proton Conductivity Measurement of the Eggshell Membrane. We calculated the proton conductivities of the Pt-coated membrane in the thickness direction using the electrochemical impedance spectra (EIS). Symmetric cells were assembled using the eggshell membranes soaked in pure water at a loading force of 3 kgf/cm^2. EIS measurements were performed using cells with the eggshell membranes on an LCR meter (HIOKI-IM3536) in the range of 1−500 kHz. We calculated the proton conductivity σ from the inverse of the resistances using the following equation:

$$\sigma = \frac{L}{RS}$$

L, R, and S are the membrane thickness, resistance, and surface area (1 × 1 cm^2), respectively.

Power Generation Performance of the Fuel Cells Using the Eggshell Membrane. The Pt-coated membrane was fixed to a current-collector board using double-sided conductive tape. First, we placed the tapes (width, 1.5 mm; length, 3 cm) on the membrane in a grid pattern (Figure S8a). We then assembled fuel cells using current-collector boards with a taped Pt-coated membrane (Figure S8b). Membrane aging was recorded using multimeters and a video camera for 120 min (Figure S8c). The open-circuit voltage V_{oc} (mV), short-circuit current I_{sc} (μA), and maximum output P_{max} (μW) were measured with a multichannel recorder at 1 min intervals to collect data for the $I-V$ curves.

An aqueous solution of carbonic acid was introduced to the anodes of the four fuel cells at 5, 10, 15, 20, 30, and 35 °C. The power output was obtained on the basis of the current and voltage recorded during the $I-V$ measurements for 120 min.

Effect of Ar/Air Switching on Electric Power Generation of the Fuel Cell. We assembled fuel cells with Ar lines connected to the cathode to test the effect of Ar or air flow on electric power generation. As shown in Figure S9, the fuel cells were encased in a box equipped with lines to alternately supply the cathode with Ar and air. The short-circuit current I_{sc} (μA), V_{oc} (mV), and $I-V$ properties were measured while passing Ar and air through the case alternately. This procedure was repeated four times.

ASSOCIATED CONTENT

Supporting Information

The Supporting Information is available free of charge at https://pubs.acs.org/doi/10.1021/acsomega.1c06687.

DSC, IR spectrum, ^{1}H MAS spectrum, ^{13}C CP MAS spectrum, diffuse reflectance spectrum, and SEM images of eggshell membrane; photographs of the eggshell membrane and fuel cells; and table of process number and chemicals to obtain the eggshell membrane (PDF)

https://doi.org/10.1021/acsomega.1c06687
ACS Omega 2022, 7, 12637−12642

AUTHOR INFORMATION

Corresponding Authors

Naoki Tanifuji − *National Institute of Technology, Yonago College, Yonago, Tottori 683-8502, Japan*; Email: tanifuji@yonago-k.ac.jp

Takeshi Shimizu − *National Institute of Technology, Yonago College, Yonago, Tottori 683-8502, Japan*; orcid.org/0000-0003-3817-7154; Email: t-shimizu@yonago-k.ac.jp

Authors

Hirofumi Yoshikawa − *School of Engineering, Kwansei Gakuin University, Sanda, Hyogo 669-1337, Japan*; orcid.org/0000-0002-0088-1579

Miki Tanaka − *National Institute of Technology, Yonago College, Yonago, Tottori 683-8502, Japan*

Kosuke Nishio − *National Institute of Technology, Yonago College, Yonago, Tottori 683-8502, Japan*; Present Address: Institute for Chemical Research, Kyoto University, Gokasho, Uji, Kyoto 611-0011, Japan

Kentaro Ida − *National Institute of Technology, Yonago College, Yonago, Tottori 683-8502, Japan*

Akihiro Shimizu − *National Institute of Technology, Yonago College, Yonago, Tottori 683-8502, Japan*

Yukio Hasebe − *ALMADO Inc., Tokyo 104-0031, Japan*

Complete contact information is available at: https://pubs.acs.org/10.1021/acsomega.1c06687

Notes

The authors declare no competing financial interest.

ACKNOWLEDGMENTS

This study was financially supported by JSPS KAKENHI (Grant No. JP 26550076 for Naoki Tanifuji, Grant No. 21K14727 for Takeshi Shimizu, Grant No. 19K22222, 20H04680, and 20H04646 for Hirofumi Yoshikawa). We also acknowledge financial support from the JSPS Core-to-Core Program A—Advanced Research Networks "International Network on Polyoxometalate Science for Advanced Functional Energy Materials" and ALMADO Inc. (2015−2018). We would like to thank Editage (www.editage.com) for English language editing.

REFERENCES

(1) Haile, S. M.; Boysen, D. A.; Chisholm, C. R. I.; Merle, R. B. Solid acids as fuel cell electrolytes. *Nature* **2001**, *410*, 910−913.

(2) Simader, G.; Vidovic, P. Success Factors for Demonstration Projects of Small-Scale Stationary Fuel Cells in Residential Buildings. *E3S Web Conf.* **2022**, *334*, 04007.

(3) Konno, N.; Mizuno, S.; Nakaji, H.; Ishikawa, Y. Development of Compact and High-Performance Fuel Cell Stack. *SAE Int. J. Altern. Powertrains* **2015**, *4* (1), 123−129.

(4) Debe, M. K. Electrocatalyst Approaches and Challenges for Automotive Fuel Cells. *Nature* **2012**, *486*, 43−51.

(5) Radenahmad, N.; Afif, A.; Petra, P. I.; Rahman, S. M. H.; Eriksson, S. G.; Azad, A. K. Proton-Conducting Electrolytes for Direct Methanol and Direct Urea Fuel Cells - A State-of-the-Art Review. *Renew. Sustain. Energy Rev.* **2016**, *57*, 1347−1358.

(6) Ay, M.; Midilli, A.; Dincer, I. Exergetic Performance Analysis of a PEM Fuel Cell. *Int. J. Energy Res.* **2006**, *30* (5), 307−321.

(7) Sun, C. J.; Chen, S. R.; Xu, G. Y.; Liu, X. M.; Yang, N. Global Variation and Uniformity of Eggshell Thickness for Chicken Eggs. *Poult. Sci.* **2012**, *91* (10), 2718−2721.

(8) Safty, S. El; Mahrose, K. M. Evaluation of Some Phenotypic, Physiological and Egg Quality Traits of African Black Neck Ostrich under Arid Desert Conditions of Libya. *Int. J. Poult. Sci.* **2009**, *8* (6), 553−558.

(9) Carvalho, J.; Araujo, J.; Castro, F. Alternative Low-Cost Adsorbent for Water and Wastewater Decontamination Derived from Eggshell Waste: An Overview. *Waste and Biomass Valorization* **2011**, *2* (2), 157−167.

(10) Banerjee, A.; Panda, S.; Sidhantha, M.; Chakrabarti, S.; Chaudhuri, B.; Bhattacharjee, S. Utilisation of Eggshell Membrane as an Adsorbent for Carbon Dioxide. *Int. J. Glob. Warm.* **2010**, *2* (3), 252−261.

(11) Torres, F. G.; Troncoso, O. P.; Montes, M. R. The Effect of Temperature on the Mechanical Properties of a Protein-Based Biopolymer Network: The Eggshell Membrane. *J. Therm. Anal. Calorim.* **2013**, *111* (3), 1921−1925.

(12) Hsieh, S.; Chou, H. H.; Hsieh, C. W.; Wu, D. C.; Kuo, C. H.; Lin, F. H. Hydrogen Peroxide Treatment of Eggshell Membrane to Control Porosity. *Food Chem.* **2013**, *141* (3), 2117−2121.

(13) Szeleszczuk, Ł.; Pisklak, D. M.; Wawer, I. Analysis of Water in the Chicken Eggshell Using the 1H Magic Angle Spinning Nuclear Magnetic Resonance Spectroscopy. *Rev. Bras. Cienc. Avic.* **2016**, *18* (spe 2), 27−32.

(14) Mathew, R.; Turdean-Ionescu, C.; Yu, Y.; Stevensson, B.; Izquierdo-Barba, I.; García, A.; Arcos, D.; Vallet-Regí, M.; Edén, M. Proton Environments in Biomimetic Calcium Phosphates Formed from Mesoporous Bioactive CaO-SiO_2-P_2O_5 Glasses in Vitro: Insights from Solid-State NMR. *J. Phys. Chem. C* **2017**, *121* (24), 13223−13238.

(15) Kodali, V. K.; Gannon, S. A.; Paramasivam, S.; Raje, S.; Polenova, T.; Thorpe, C. A Novel Disulfide-Rich Protein Motif from Avian Eggshell Membranes. *PLoS One* **2011**, *6* (3), e18187.

(16) Pisklak, D. M. I.; Szeleszczuk, Ł.; Wawer, I. 1H and 13C Magic-Angle Spinning Nuclear Magnetic Resonance Studies of the Chicken Eggshell. *J. Agric. Food Chem.* **2012**, *60* (50), 12254−12259.

(17) Baker, J. R.; Balch, D. A. A Study of the Organic Material of Hen's-Egg Shell. *Biochem. J.* **1962**, *82* (1956), 352−361.

(18) Ordinario, D. D.; Phan, L.; Walkup, W. G., IV; Jocson, J. M.; Karshalev, E.; Hüsken, N.; Gorodetsky, A. A. Bulk Protonic Conductivity in a Cephalopod Structural Protein. *Nat. Chem.* **2014**, *6* (7), 596−602.

(19) Li, Y.; Ye, Y.; Fan, Y.; Zhou, J.; Jia, L.; Tang, B.; Wang, X. Silver Nanoprism-Loaded Eggshell Membrane: A Facile Platform for in Situ SERS Monitoring of Catalytic Reactions. *Crystals* **2017**, *7* (2), 45.

(20) Kim, W. D.; Min, T.; Park, S. A.; Park, J. H.; Kim, G. H. A Natural and Biodegradable Scaffold of Electrospun Eggshell Membrane. *WIT Trans. Eng. Sci.* **2007**, *57*, 349−358.

(21) Molavian, M. R.; Abdolmaleki, A.; Gharibi, H.; Firouz Tadavani, K.; Zhiani, M. Safe and Green Modified Ostrich Eggshell Membranes as Dual Functional Fuel Cell Membranes. *Energy Fuels* **2017**, *31* (2), 2017−2023.

(22) Bayer, T.; Cunning, B. V.; Selyanchyn, R.; Nishihara, M.; Fujikawa, S.; Sasaki, K.; Lyth, S. M. High Temperature Proton Conduction in Nanocellulose Membranes: Paper Fuel Cells. *Chem. Mater.* **2016**, *28* (13), 4805−4814.

(23) Sone, Y.; Ekdunge, P.; Simonsson, D. Proton Conductivity of Nafion 117 as Measured by a Four-Electrode AC Impedance Method. *J. Electrochem. Soc.* **1996**, *143* (4), 1254−1259.

(24) Falk, M. An Infrared Study of Water in Perfluorosulfonate (Nafion) Membranes. *Can. J. Chem.* **1980**, *58* (14), 1495−1501.

(25) Chen, X.; Zhu, L.; Wen, W.; Lu, L.; Luo, B.; Zhou, C. Biomimetic Mineralisation of Eggshell Membrane Featuring Natural Nanofiber Network Structure for Improving Its Osteogenic Activity. *Colloids Surfaces B Biointerfaces* **2019**, *179*, 299−308.

(26) Steele, B. C. H.; Heinzel, A. Materials for fuel-cell technologies. *Nature* **2001**, *414*, 345−352.

(27) Chu, S.; Majumdar, A. Opportunities and Challenges for a Sustainable Energy Future. *Nature* **2012**, *488*, 294−303.

(28) Newton, M. A.; Ferri, D.; Smolentsev, G.; Marchionni, V.; Nachtegaal, M. Kinetic Studies of the Pt Carbonate-Mediated, Room-Temperature Oxidation of Carbon Monoxide by Oxygen over Pt/

Al2O3 Using Combined, Time-Resolved XAFS, DRIFTS, and Mass Spectrometry. *J. Am. Chem. Soc.* **2016**, *138* (42), 13930−13940.

https://doi.org/10.1021/acsomega.1c06687
ACS Omega 2022, 7, 12637−12642